Exploration of electromagnetic outflows of inspiraling binary neutron stars

Dimitrios Skiathas
SURA, NASA GSFC, University of Patras

Constantinos Kalapotharakos, *NASA GSFC*
Zorawar Wadiasingh, *NASA GSFC, UMD*
Demos Kazanas, *NASA GSFC*
Alice Harding, *LANL*
Paul Kolbeck, *UW*

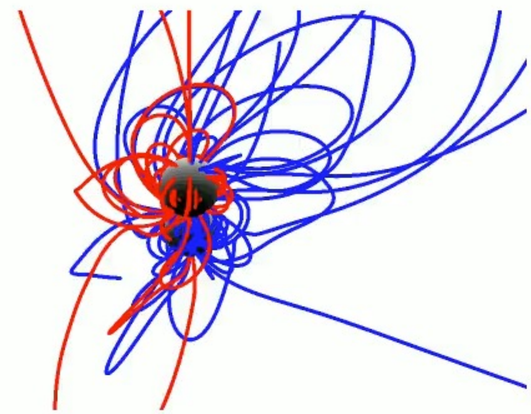

Introduction

- Interacting neutron star magnetospheres can release large amount of energy through electromagnetic emissions.

Piro 2012, Tsang et al. 2012 , Pelenzuela et al. 2013, Lyutikov 2019, Sridhar et al. 2021, Most & Philippov 2020,2022 , Cooper et al 2023

- Precursor signal to neutron star mergers.

- Echoes contributing to the GRB afterglows.

- Our goal is to explore the parameter space regarding the emission patterns.

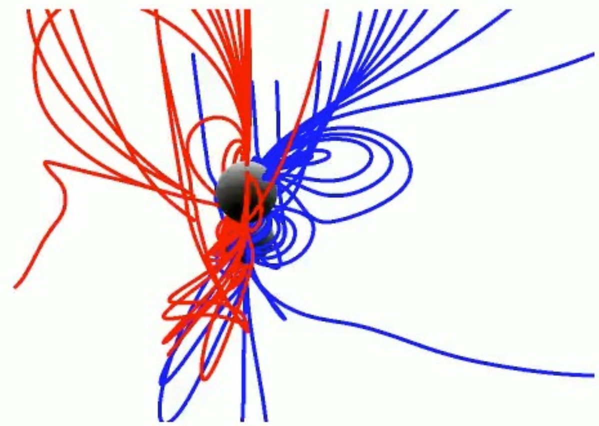

For a review see Suvorov et al. 2024

Assuming emissions due to CR at the radiation reaction limit regime

See Kalapotharakos et al. 2014, 2017, 2022

and Konstantinos Poster about the Fundamental Plane

$$\frac{d\gamma_L}{dt} = \frac{q_e v E_{acc}}{m_e c^2} - \frac{2 q_e \gamma_L^4}{3 R_c^2 m_e c} = 0, \text{with } \mathrm{E_{acc}} \sim \mathrm{B_{LC}} \text{ and } \mathrm{R_c} \sim \mathrm{R_{LC}}$$

The cut off energy $\epsilon_{cut} = \frac{3}{2} c\hbar \frac{\gamma_L^3}{R_c}$

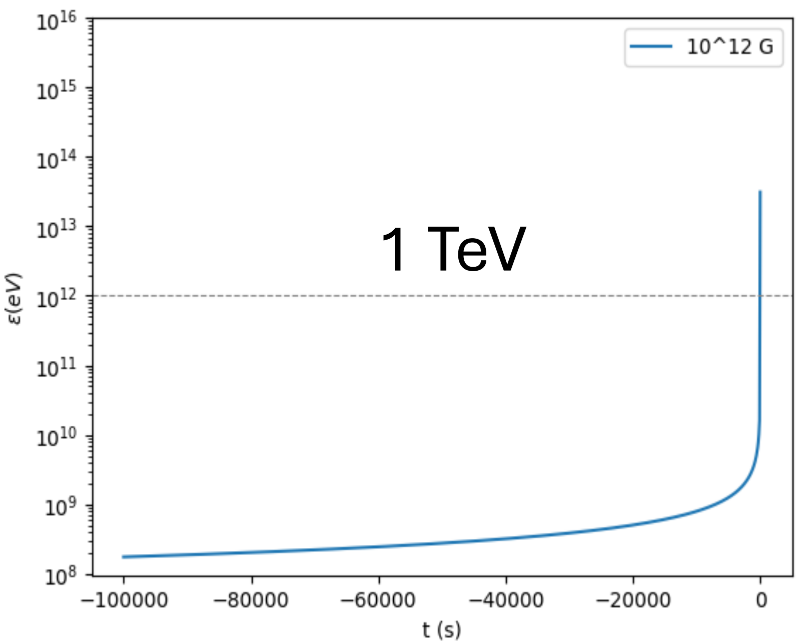

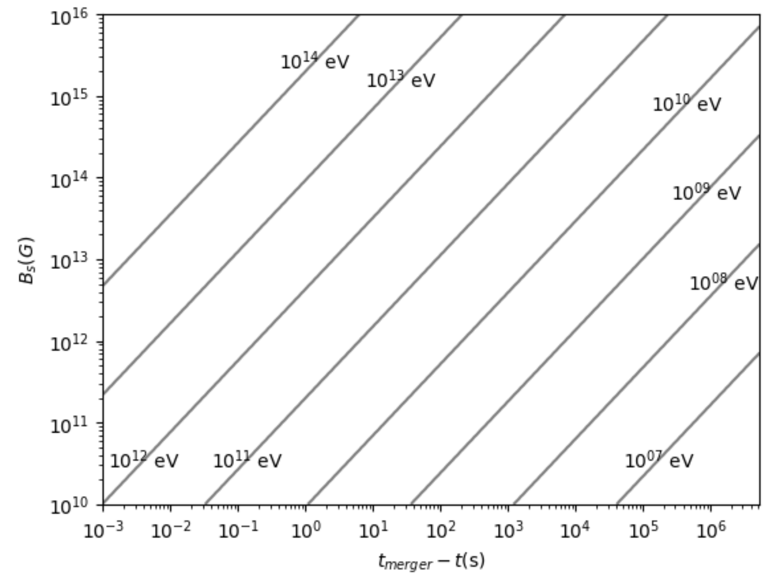

Likely detectable with CTA with warnings from 3G GW detectors (~2030s)

Assuming emissions due to CR at the radiation reaction limit regime

$$\frac{d\gamma_L}{dt} = \frac{q_e v E_{acc}}{m_e c^2} - \frac{2 q_e \gamma_L^4}{3 R_c^2 m_e c} = 0, \text{with } \mathrm{E_{acc}} \sim \mathrm{B_{LC}} \text{ and } \mathrm{R_c} \sim \mathrm{R_{LC}}$$

The cut off energy $\epsilon_{cut} = \frac{3}{2} c\hbar \frac{\gamma_L^3}{R_c}$

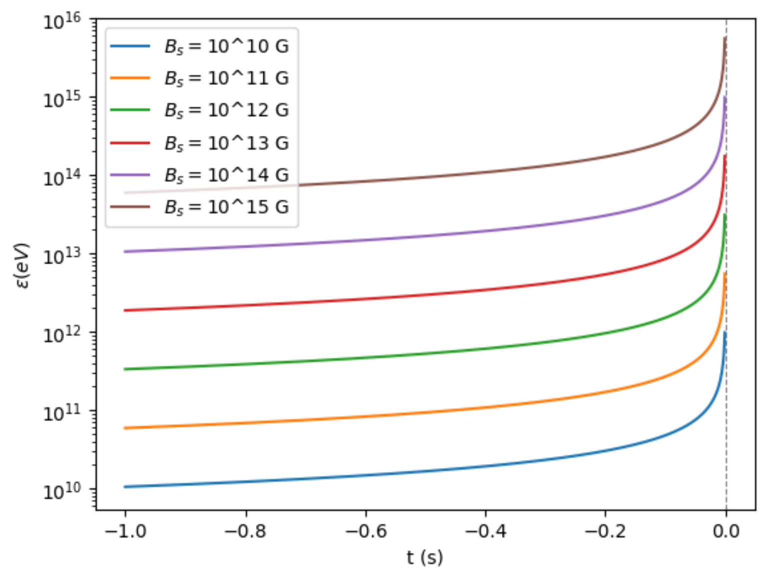

See Kalapotharakos et al. 2014, 2017, 2022

and Konstantinos Poster about the Fundamental Plane

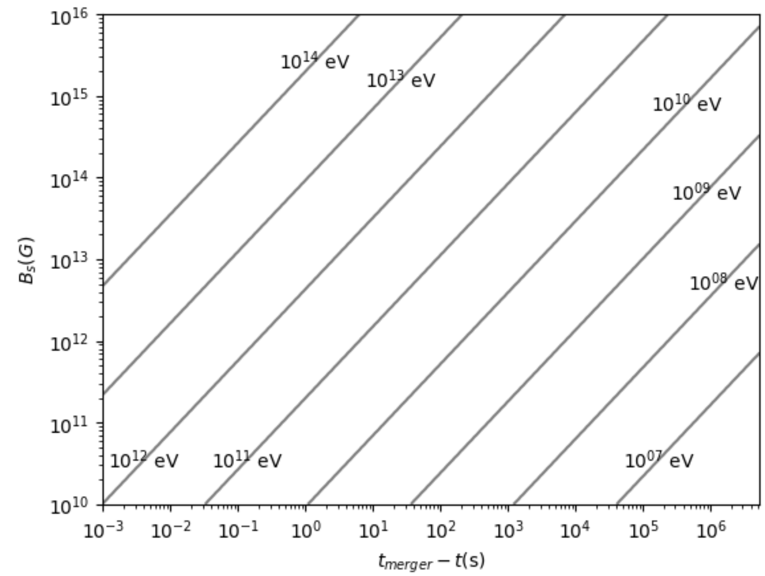

Likely detectable with CTA with warnings from 3G GW detectors (~2030s)

Introduction

- Interacting neutron star magnetospheres can release large amount of energy through electromagnetic emissions.

Piro 2012, Tsang et al. 2012 , Pelenzuela et al. 2013, Lyutikov 2019, Sridhar et al. 2021, Most & Philippov 2020,2022 , Cooper et al 2023

- Precursor signal to neutron star mergers.
- Echoes contributing to the GRB afterglows.
- Our goal is to explore the parameter space regarding the emission patterns.

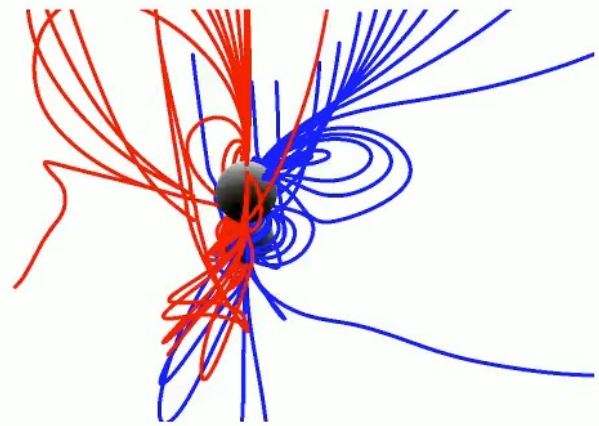

For a review see Suvorov et al. 2024

Echoes:

$$\Delta t \simeq \frac{l - d}{c}$$
$$= \frac{l}{c}(1 - cos\theta)$$

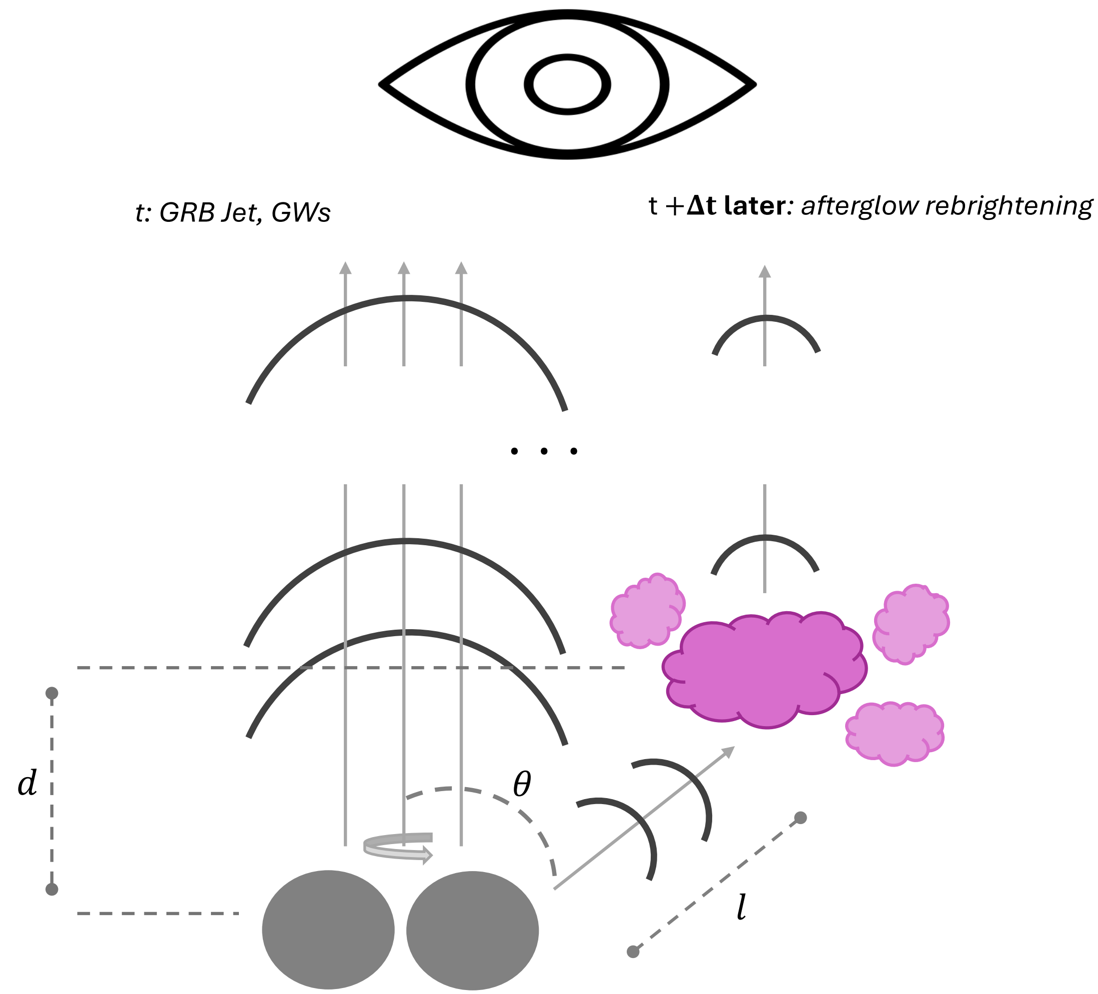

Introduction

- Interacting neutron star magnetospheres can release large amount of energy through electromagnetic emissions.

  Piro 2012, Tsang et al. 2012 , Pelenzuela et al. 2013, Lyutikov 2019, Sridhar et al. 2021, Most & Philippov 2020,2022 , Cooper et al 2023

- Precursor signal to neutron star mergers.

- Creating echoes contributing to the GRB afterglows.

- Our goal is to explore the parameter space regarding the emission patterns.

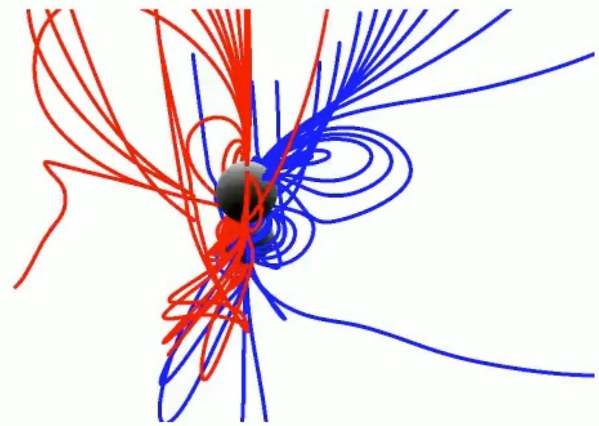

For a review see Suvorov et al. 2024

Exploration parameters

- Inclination angle of the 1st star

  a_1: $0°, 45°, 90°$

- Inclination angle of the 2nd star

  a_2: $0°, 45°, 90°$

- Ratio of their magnetic moments

  $b_1/b_2 : -10^2, -10, -10^{\frac{1}{2}}$, -1, 1, $10^{\frac{1}{2}}$, $10, 10^2$

- Spin phase difference*

  $\Delta\phi$: $0°, 45°, 90°$

Only for some b_1/b_2 ratio

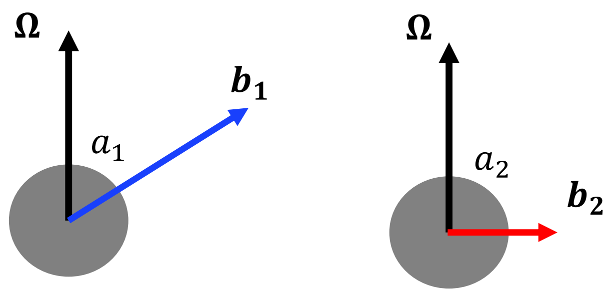

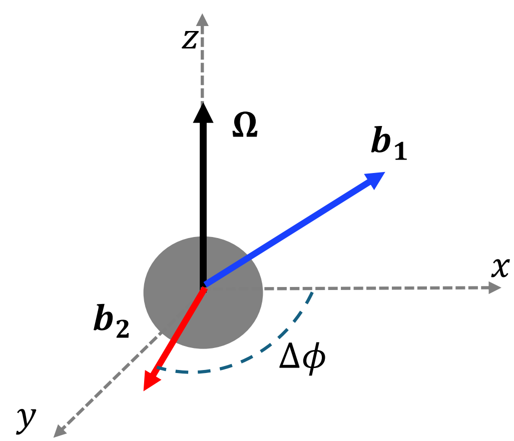

Our approach

- In the limit of irrotational stars: $\omega_1 = \omega_2 = 0$.
- Dipole magnetic moments.
- Two neutron stars with $R_* = 12km$ and $M_* = 1.4\ M_\odot$
- $\Omega = \left(1 - \frac{t}{t_s}\right)^{-3/8}$ with t_s the time to the merger.

Medvedev & Loeb 2013, Peters 1964

- $\frac{r}{r_i} = \left(\frac{\Omega}{\Omega_i}\right)^{-2/3}$

Our approach

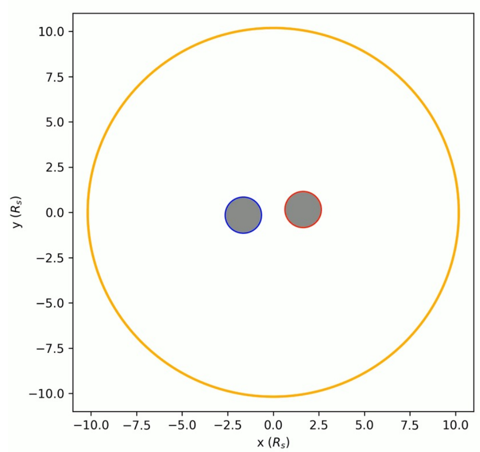

- In the limit of irrotational stars: $\omega_1 = \omega_2 = 0$.
- Dipole magnetic moments.
- Two neutron stars with $R_* = 12km$ and $M_* = 1.4\ M_\odot$
- $\Omega = \left(1 - \frac{t}{t_s}\right)^{-3/8}$ with t_s the time to the merger.

Medvedev & Loeb 2013, Peters 1964

- $\frac{r}{r_i} = \left(\frac{\Omega}{\Omega_i}\right)^{-2/3}$

Our approach

- Ignoring tidal distortions and crust cracking.
- Numerical 3D force-free MHD simulation of global magnetosphere.

Kalapotharakos et al. (2012)

- Grid size: ~ 500x500x500.
- Initial separation $d = 3.3R_*$.
- Simulations last for 7.7 ms (**4 rotations**) until neutron stars touch.

Example Run for ~50 Rotations

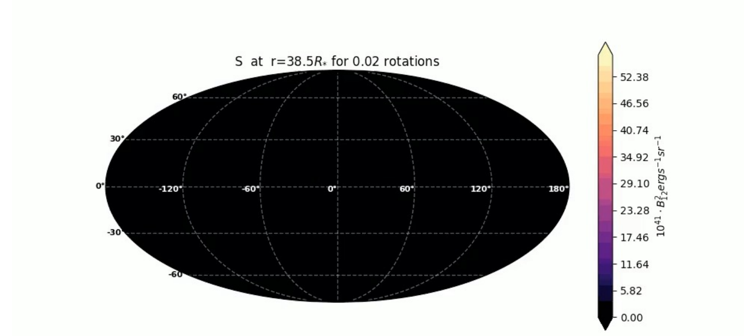

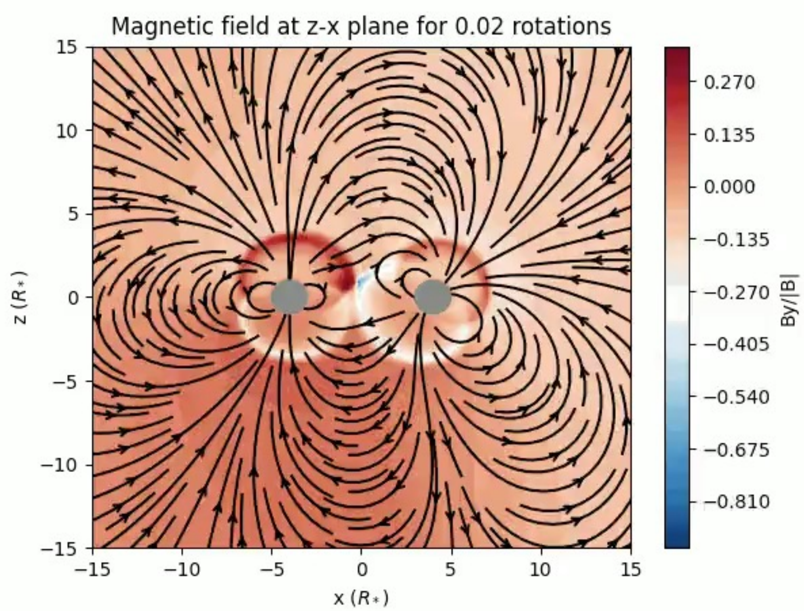

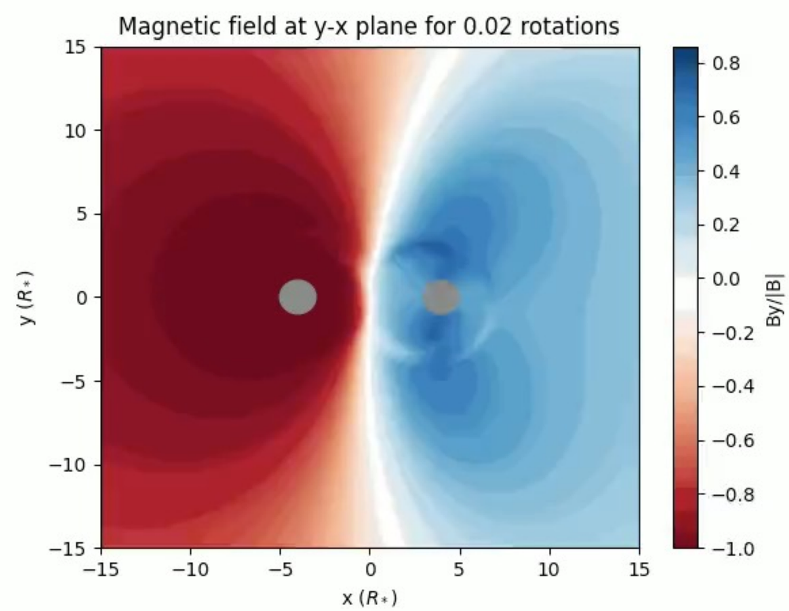

Single Isolated Pulsar

Energy Flux: $L = \int \boldsymbol{S} \cdot d\boldsymbol{A},$ where $\boldsymbol{S} = \frac{c}{4\pi} \boldsymbol{E} \times \boldsymbol{B},$ the Poynting vector.

the directional energy flux per time and area unit

For dipole magnetic moment: $L \propto \mu^2 \omega^4 / c^3$

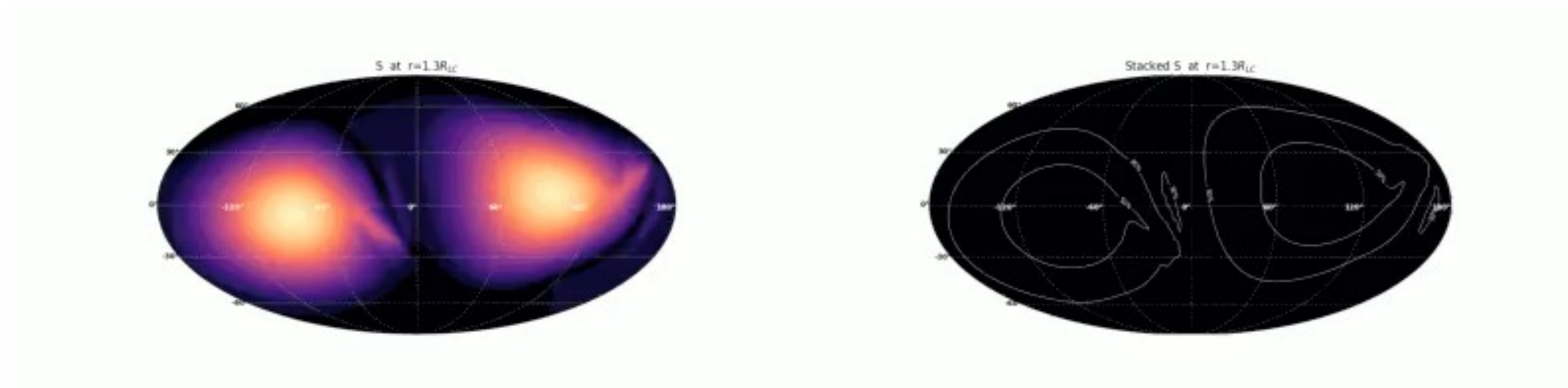

Single Isolated Pulsar

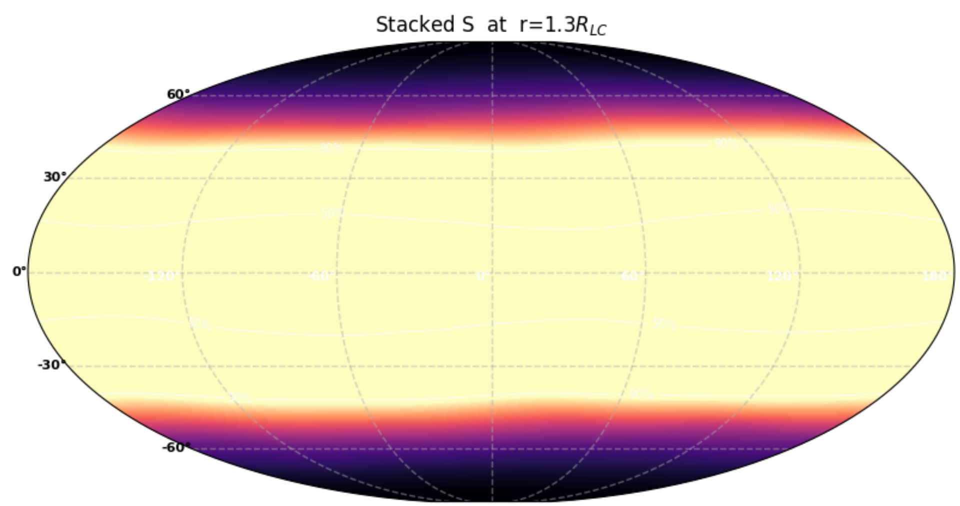

...only θ matters!

144 cases explored

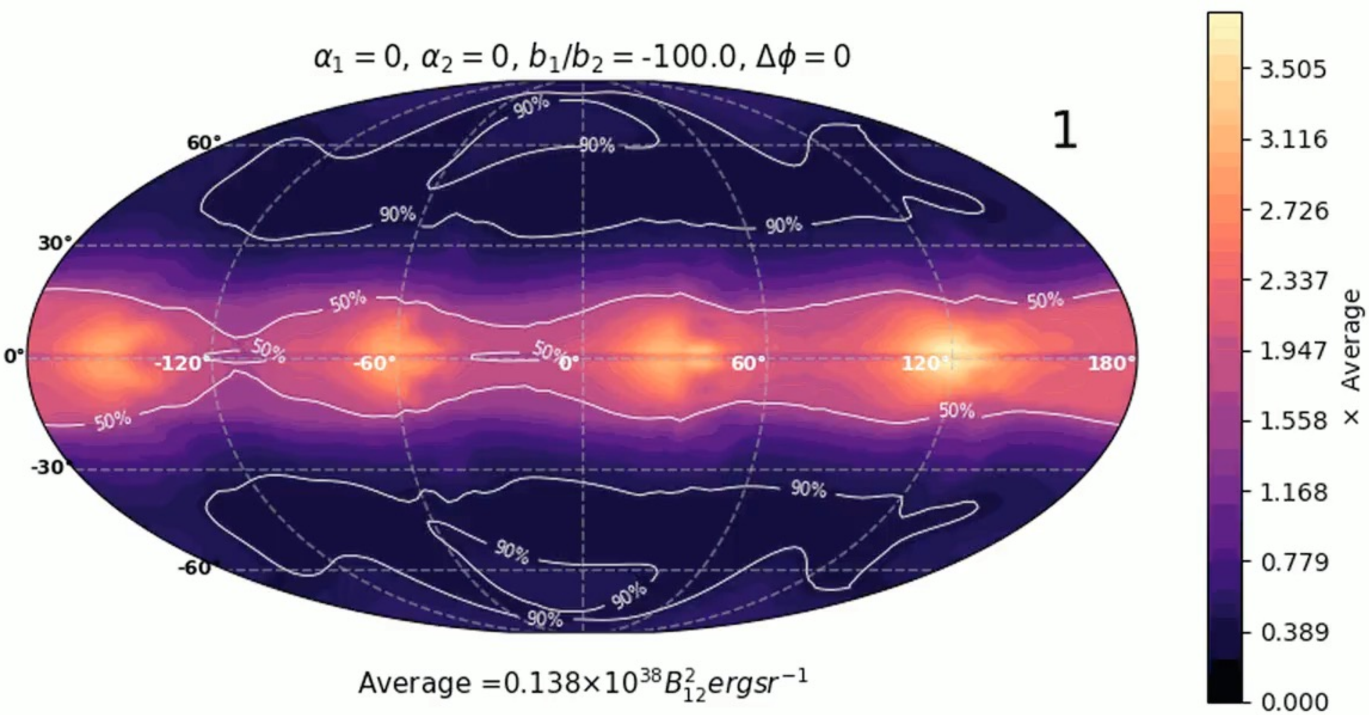

Both θ and ϕ matters

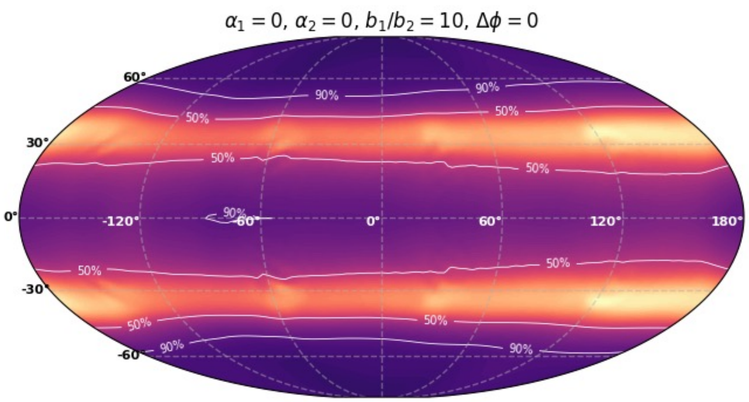

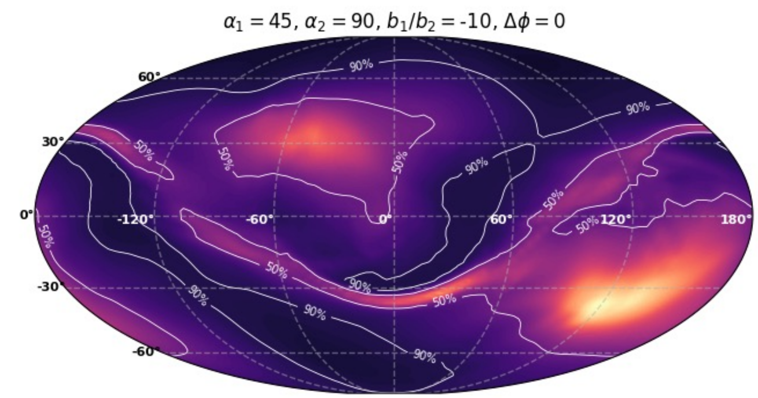

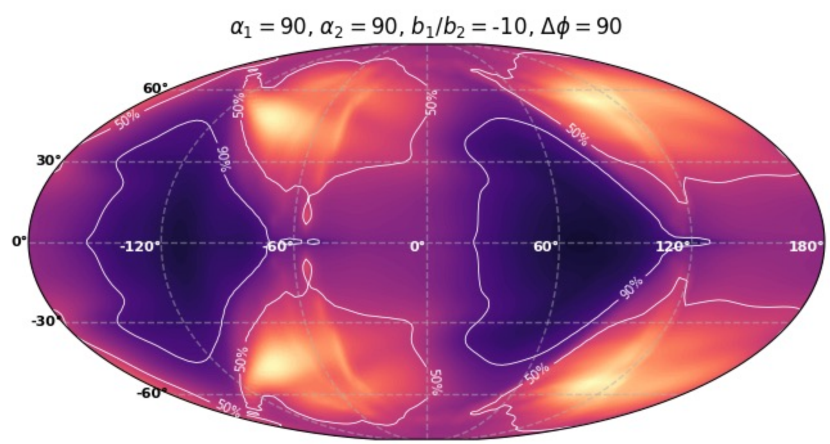

Aligned

$\boldsymbol{\alpha_1 = 0°, a_2 = 0°, b_2 = b_1}$

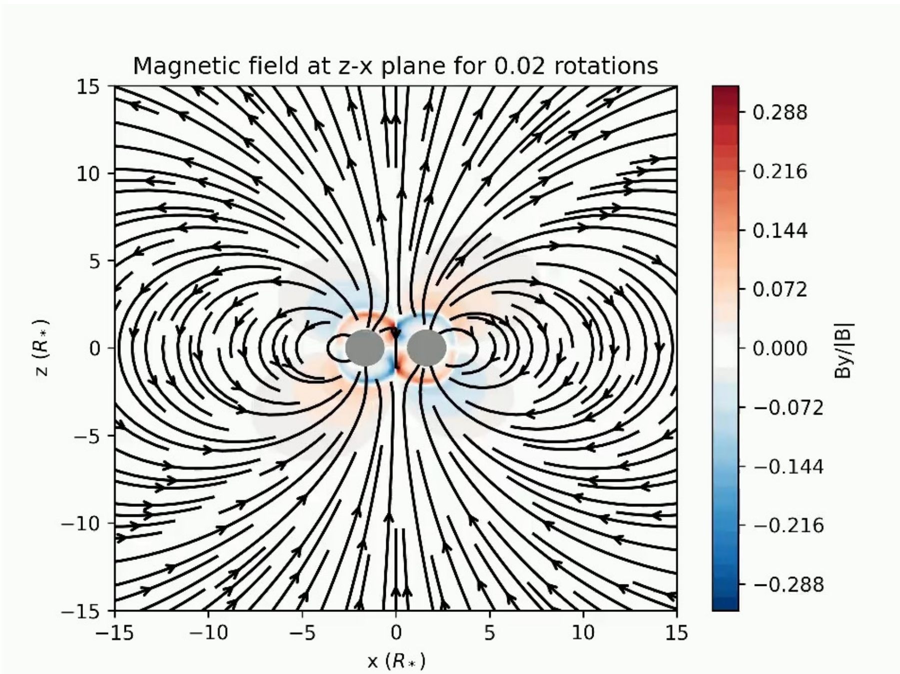

Anti-Aligned

$\boldsymbol{\alpha_1 = 0°, a_2 = 0°, b_2 = -b_1}$

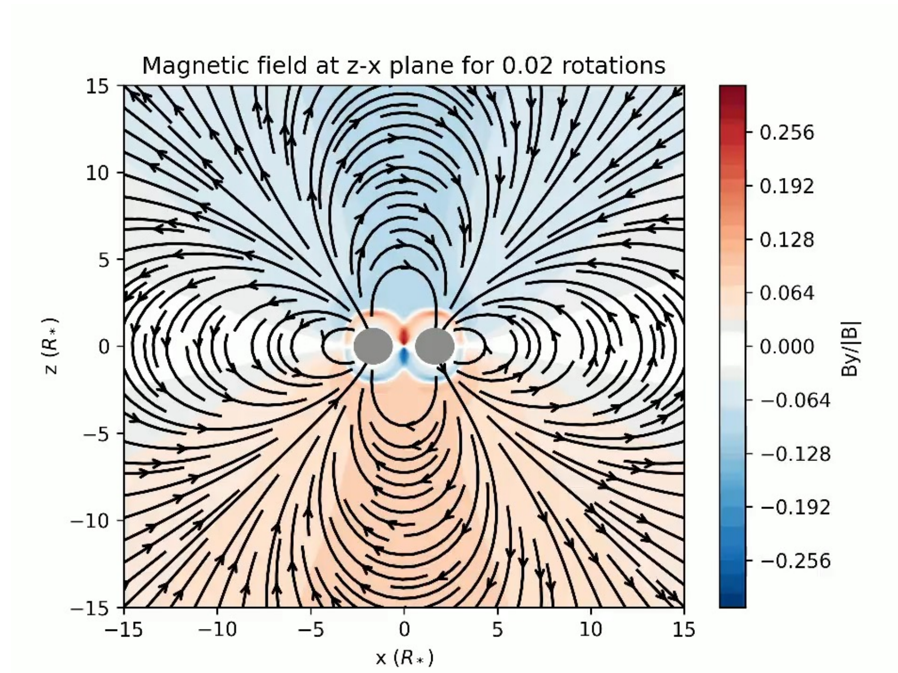

Aligned vs Anti-Aligned

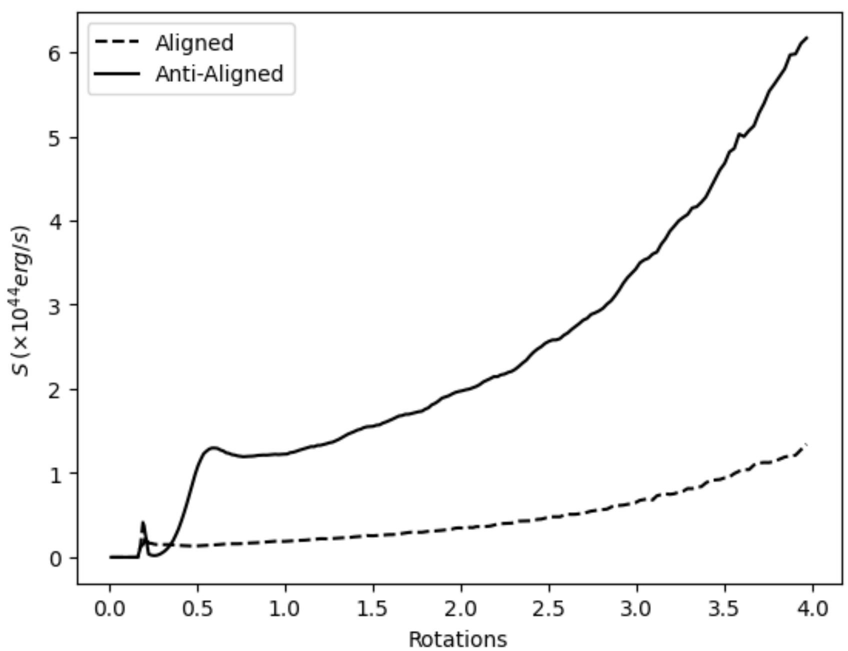

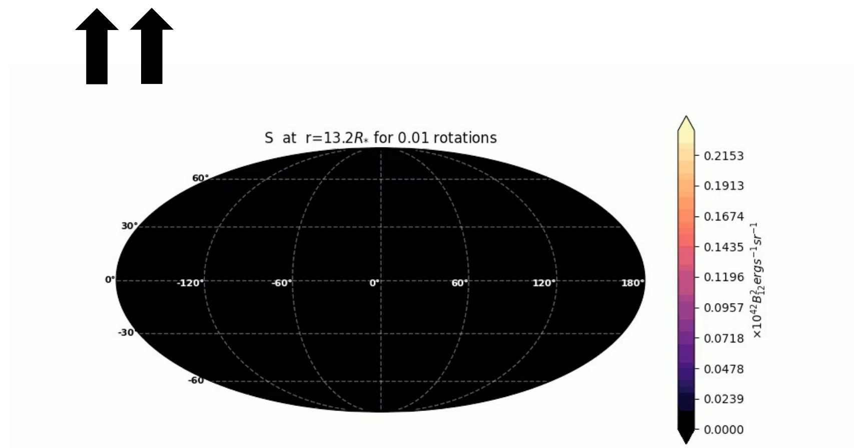

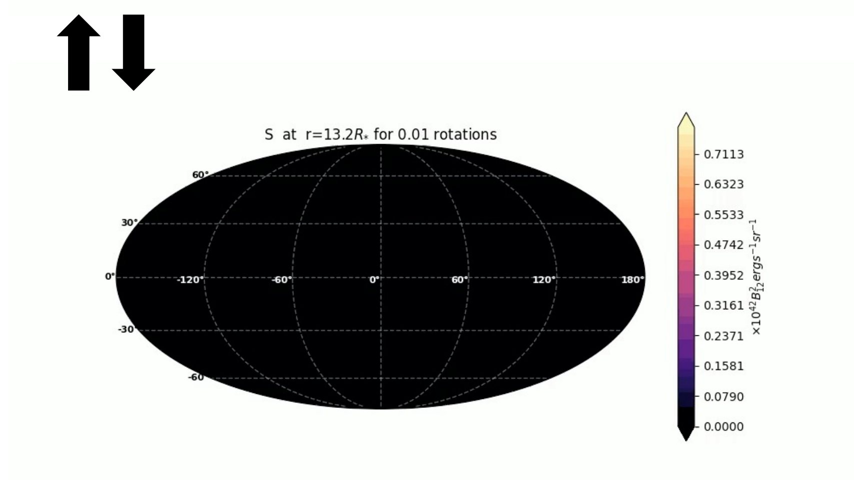

Consistent with *Most & Philippov 2020,2022 and Pelenzuella et al. 2013*

Inclination angles

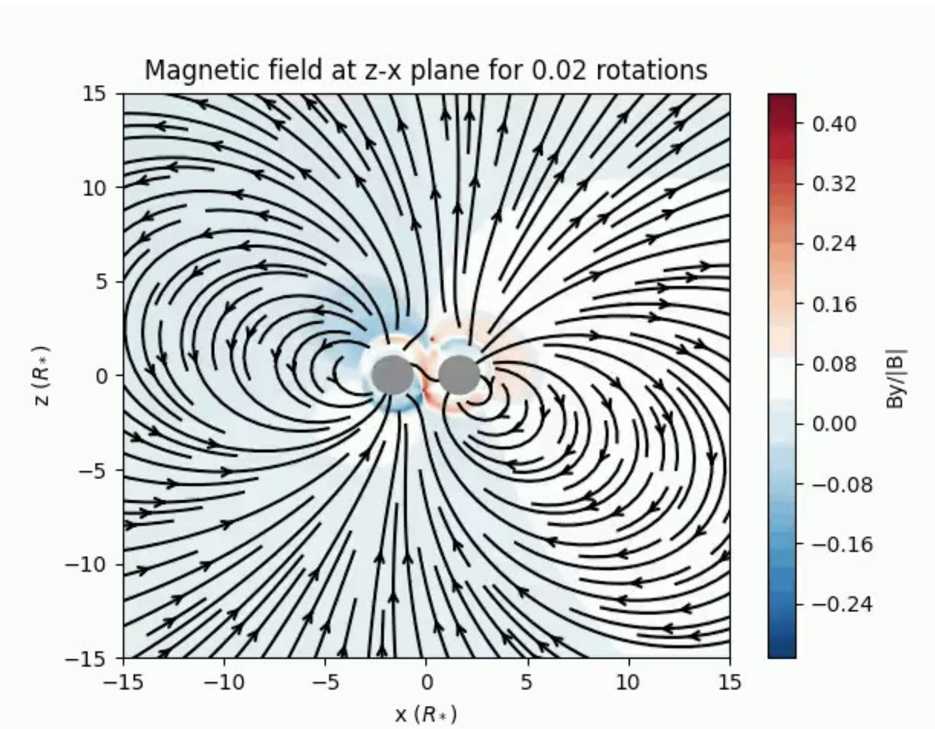

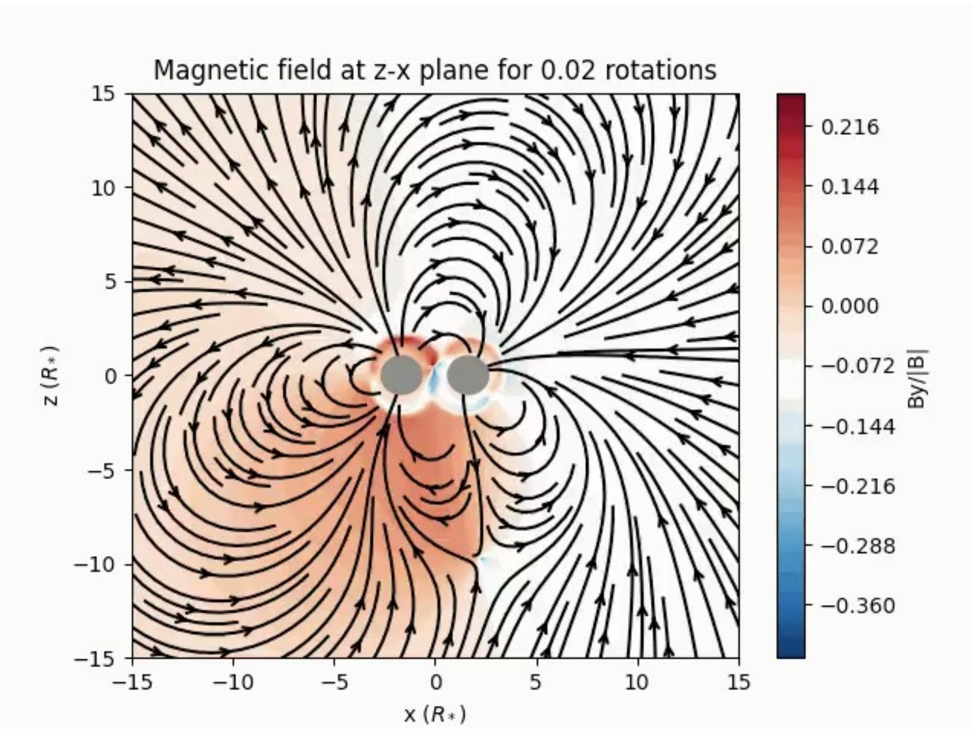

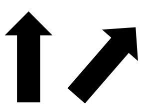

$\boldsymbol{\alpha_1 = 0°, a_2 = 45°, b_2 = b_1}$

$\boldsymbol{\alpha_1 = 0°, a_2 = 45°, b_2 = -b_1}$

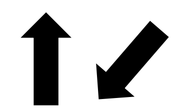

Inclination angles

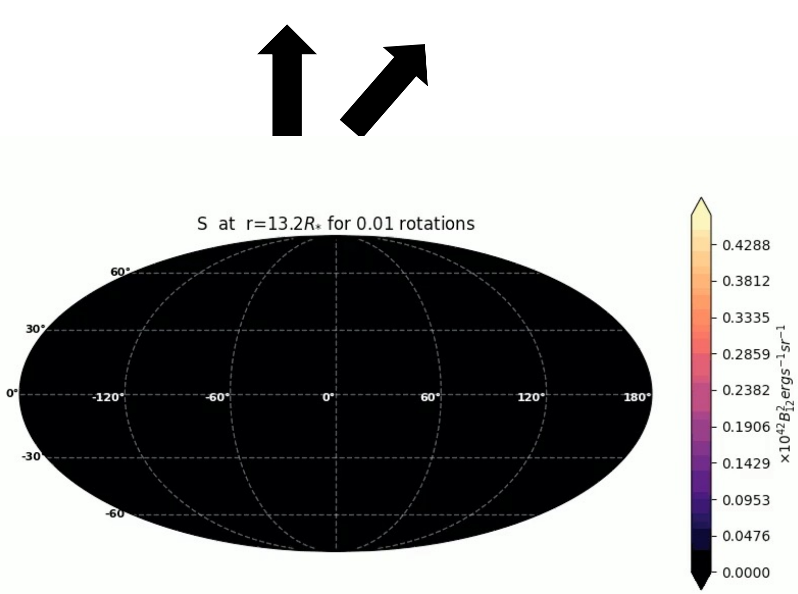

$\boldsymbol{\alpha_1 = 0°, a_2 = 45°, b_2 = b_1}$

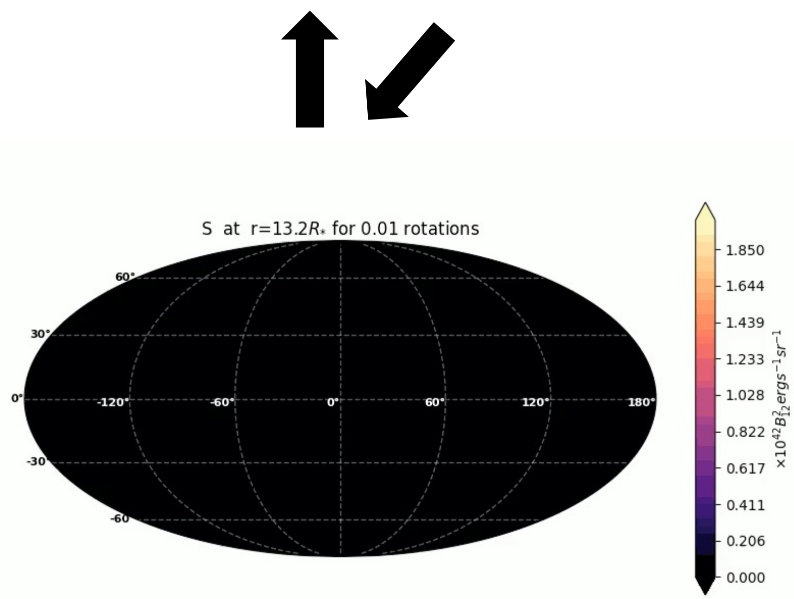

$\boldsymbol{\alpha_1 = 0°, a_2 = 45°, b_2 = -b_1}$

Effect of inclination angles:

Aligned stars with inclination give more flux

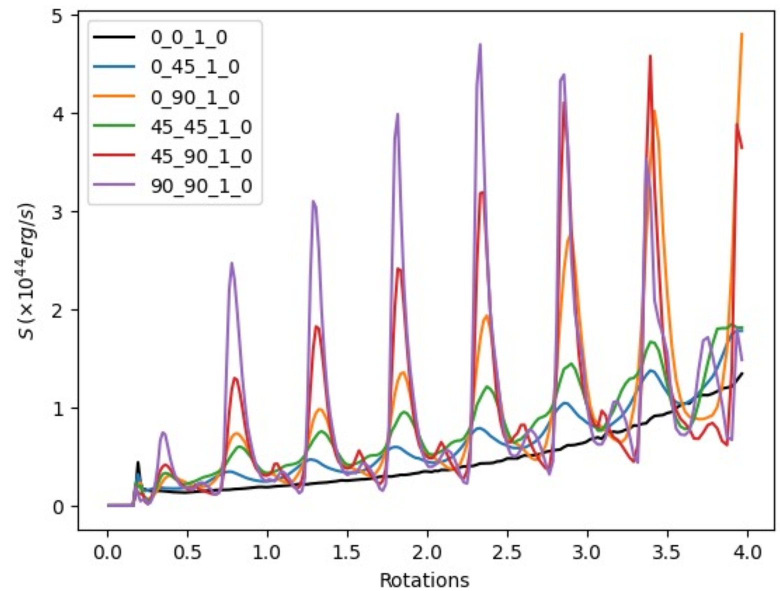

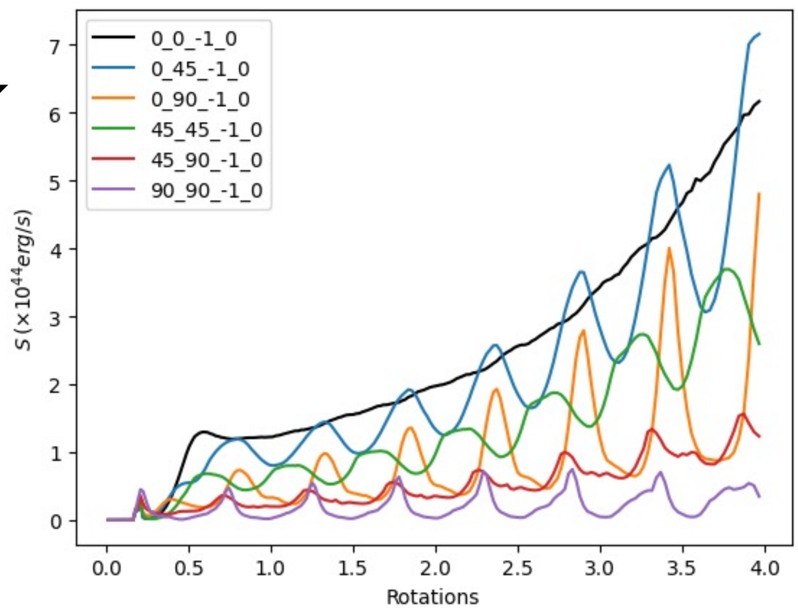

Anti - aligned stars with inclination give less flux

Torques and kicks

Due to asymmetric pointing flux torques and kicks might develop that will might affect the orbit or magnetic alignment.

$$\boldsymbol{f} = \boldsymbol{\nabla} \cdot \boldsymbol{\sigma} - \frac{1}{c^2}\frac{\partial \boldsymbol{S}}{\partial t}$$

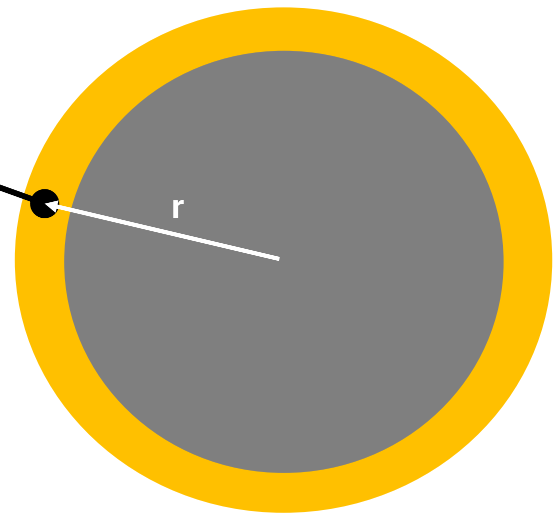

Where σ is the Maxwell tensor:

$$\sigma_{ij} = \frac{1}{4\pi}\left(E_i E_j + B_i B_j - \frac{1}{2}(E^2 + B^2)\delta_{ij}\right)$$

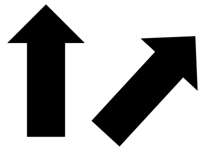

$\alpha_1 = 0°, \alpha_2 = 45°$

F=6.20e+28N, Fx=2.48e+28N, Fy=-3.07e+28N, Fz=4.77e+28N,
F1=4.18e+29N, F1x=-3.63e+29N, F1y=1.14e+29N, F1z=-1.73e+29N,
F2=4.69e+29N, F2x=3.88e+29N, F2y=-1.45e+29N, F2z=2.21e+29N,

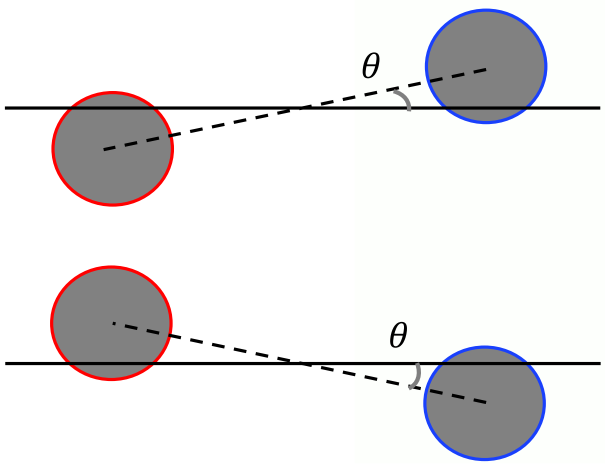

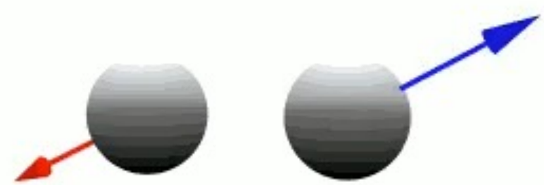

For $3.16\times10^{15}G$: $\frac{F_{EM}}{F_G} \leq 10^{-3}$

Potentially important for 3G GW detectors.

Effect of b_1/b_2 ratio:

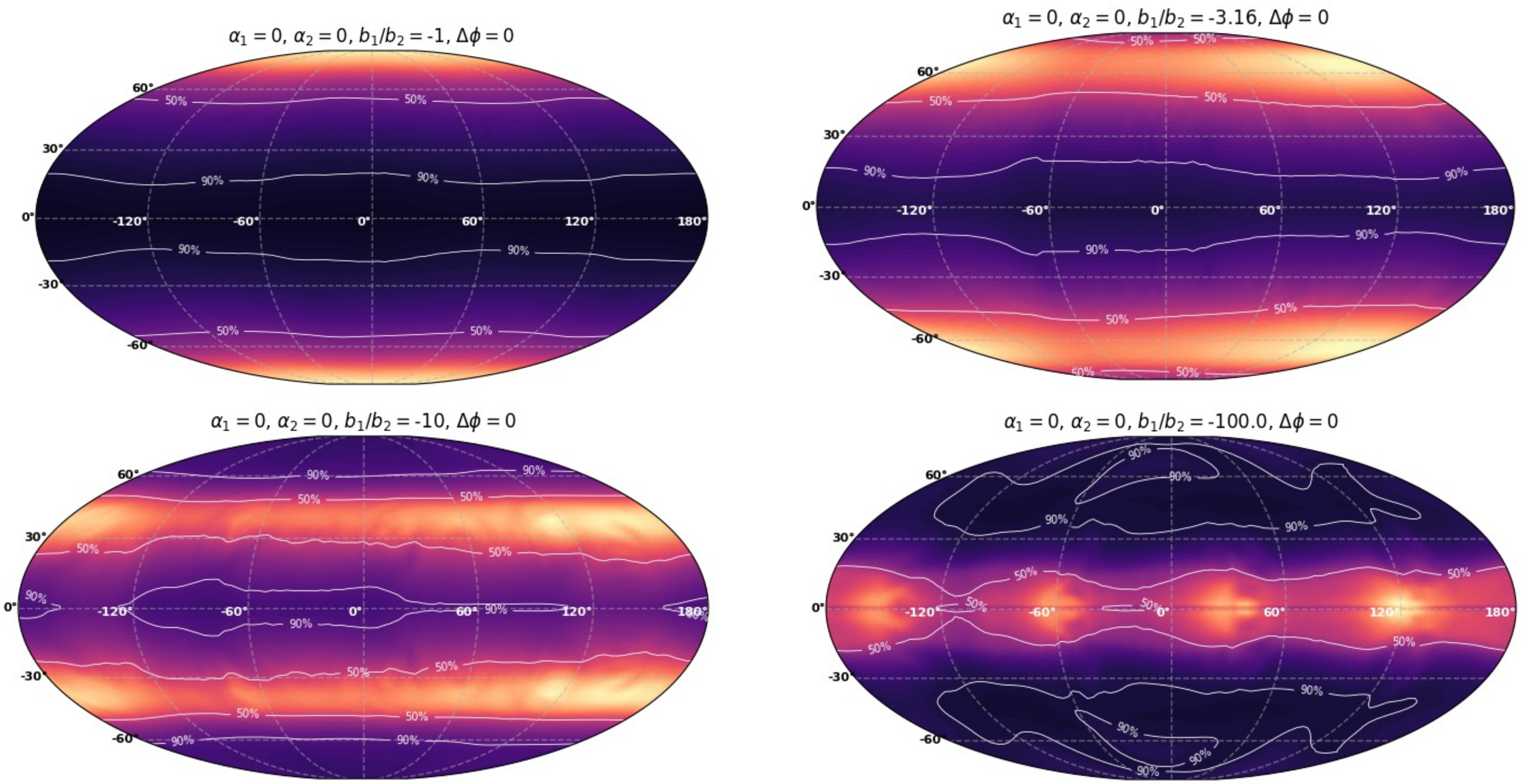

Poynting flux dependency on Ω.

$$L \sim \boldsymbol{\Omega}^{\boldsymbol{n}} \cdot f\left(\alpha_1, \alpha_2, \Delta\phi\right)$$

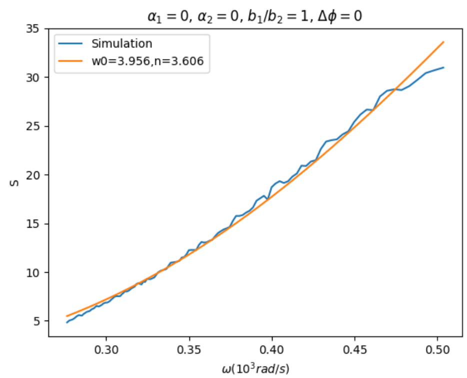

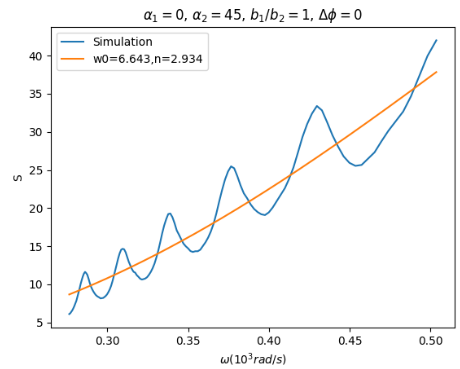

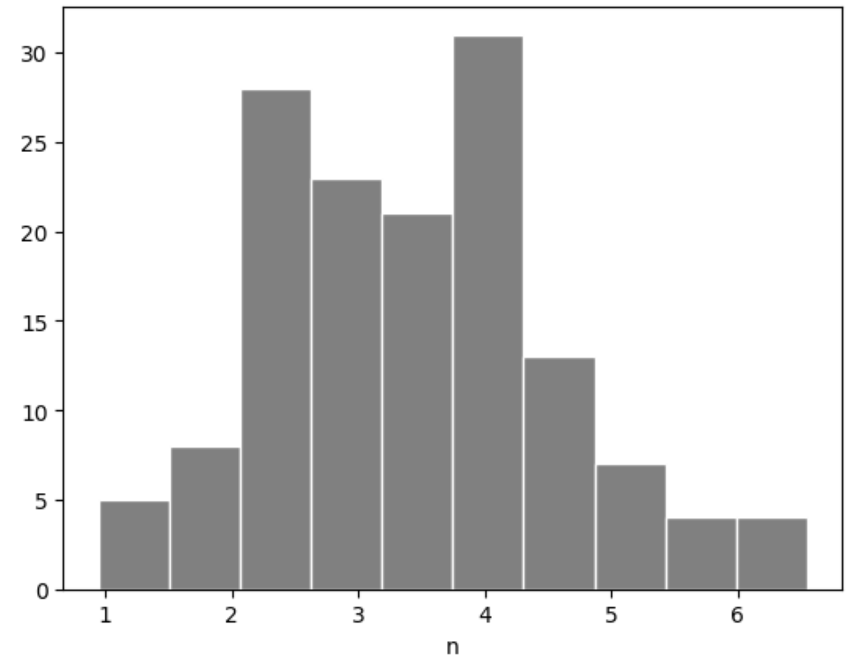

For single isolated pulsar n=4

Poynting flux dependency on Ω.

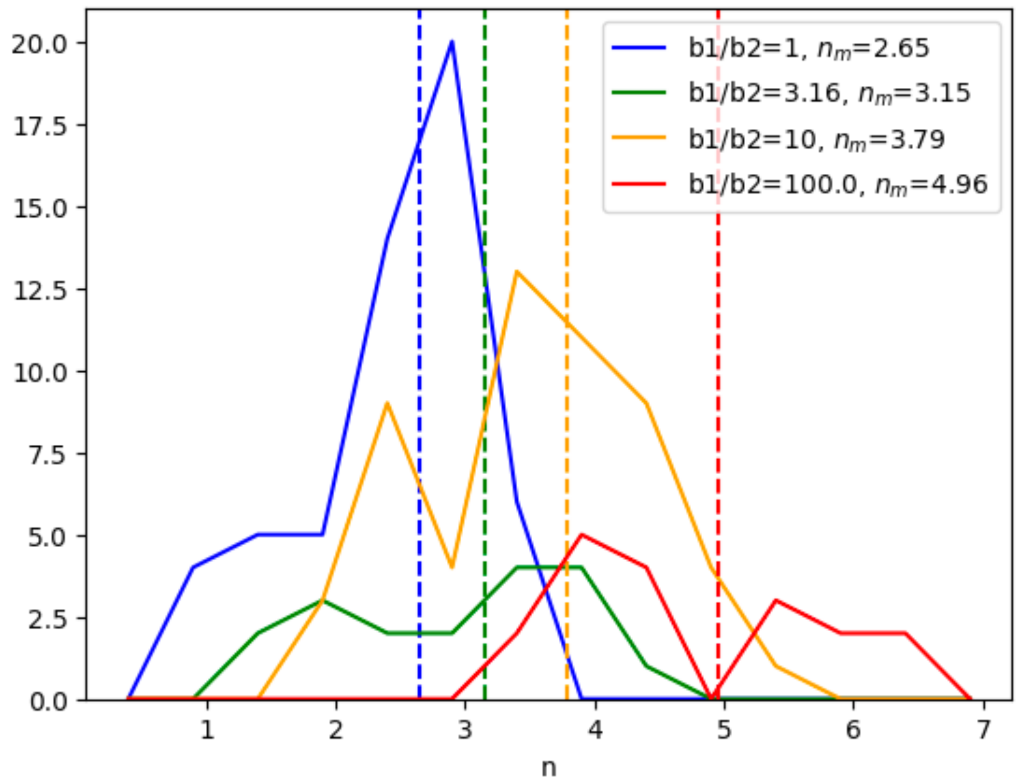

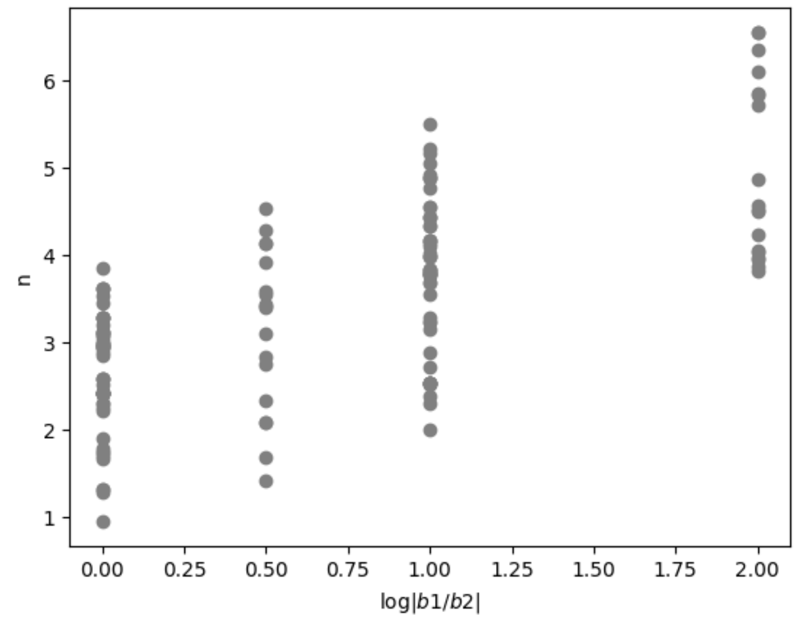

γ – rays patterns

- Acceleration of particles from $E_{||}$ and emission of high energy photons.
- $\boldsymbol{E}_{||} = \frac{c|(\nabla\times\boldsymbol{B})_{||}|}{4\pi\sigma}$
- Emissions happen in the region outside the orbital light cylinder at points where $\boldsymbol{E}_{||}$ is high.
- Emission from each point contribute at the direction of particle's velocity on the appropriate time considering the time delay.
- Luminosity is considered as a function of the Poynting flux with a distance depended efficiency.

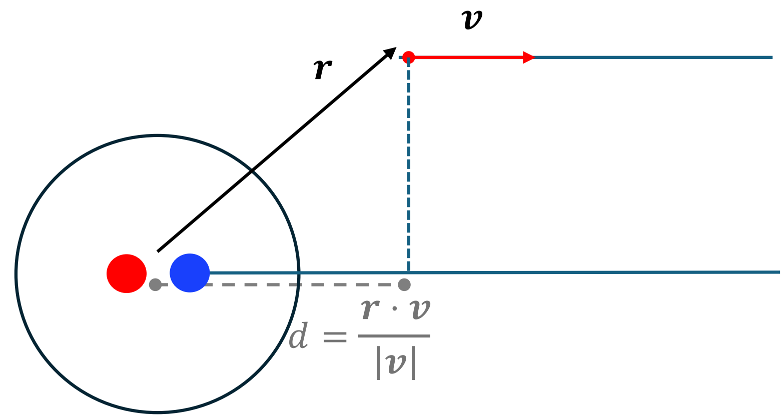

$$\boldsymbol{v} = \frac{\boldsymbol{E}\times\boldsymbol{B} \pm (B_0\boldsymbol{B} + E_0\boldsymbol{E})}{B^2 + E_0^2}$$

Gruzinov 2012
Kalapotharakos et al. 2014
Brambilla et al. 2015

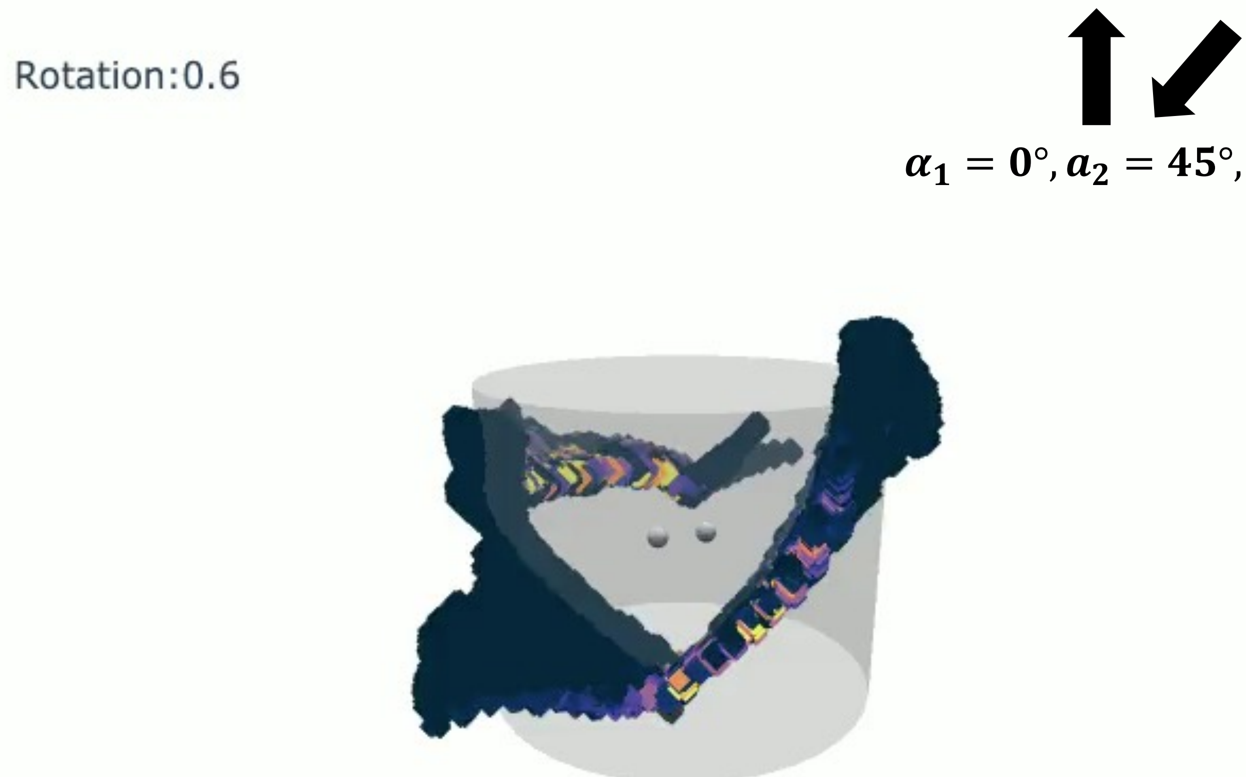

$\boldsymbol{\alpha_1 = 0°, a_2 = 45°, b_1 = -b_2}$

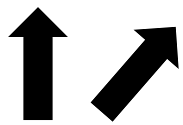

$\alpha_1 = 0°, a_2 = 45°, b_1 = b_2$

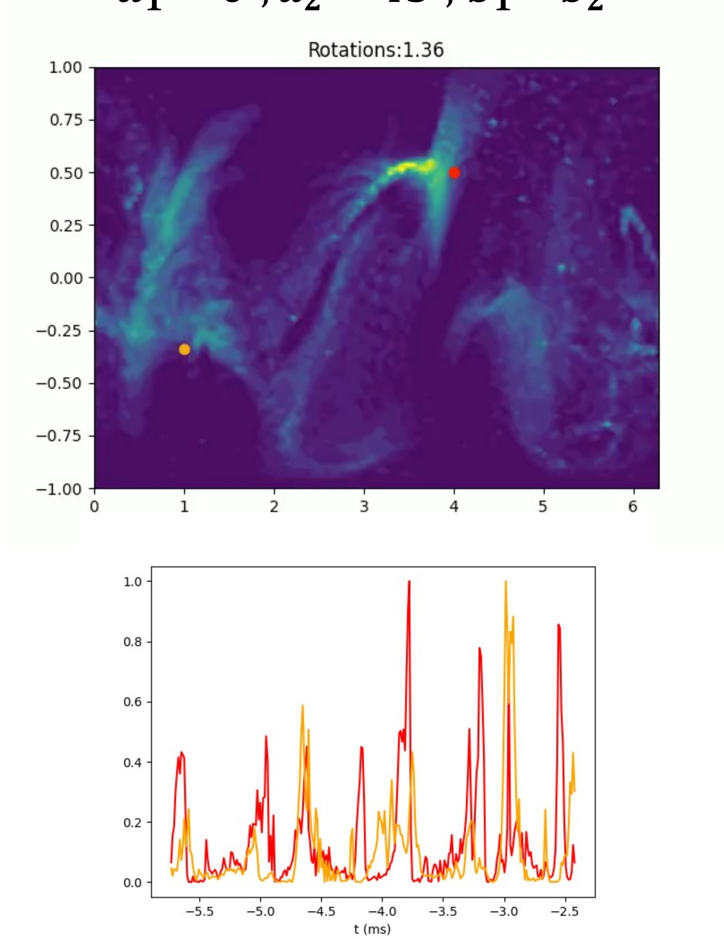

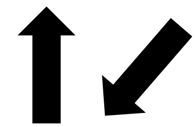

$\alpha_1 = 0°, a_2 = 45°, b_1 = -b_2$

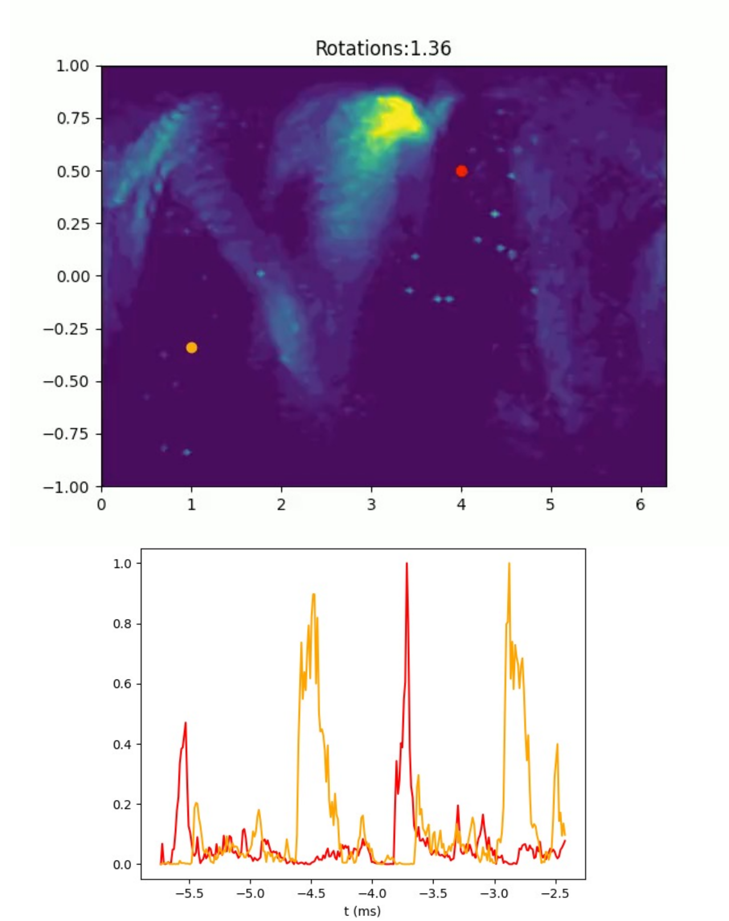

Conclusions

- We explored the parameter space of binary neutron star mergers and their precursor emissions.

144 cases

- The flux varies a lot:

$\sim \mathbf{10^{42} - 10^{45} B_{12}^2 ergs^{-1}}$

or $\sim \mathbf{10^{49} - 10^{52} B_{15.5}^2 ergs^{-1}}$

- If $L_\gamma < 10\% L_{Poynting}$ γ −rays might be detectable from CTA.
- Non uniform flux distribution over the sky.

50% in less than ~1/3 of the sky

- The Poynting flux dependency on Ω varies.
- Having inclination angles results in different behavior for the aligned and anti-aligned cases and potentially implications on the orbits.

Thank you!

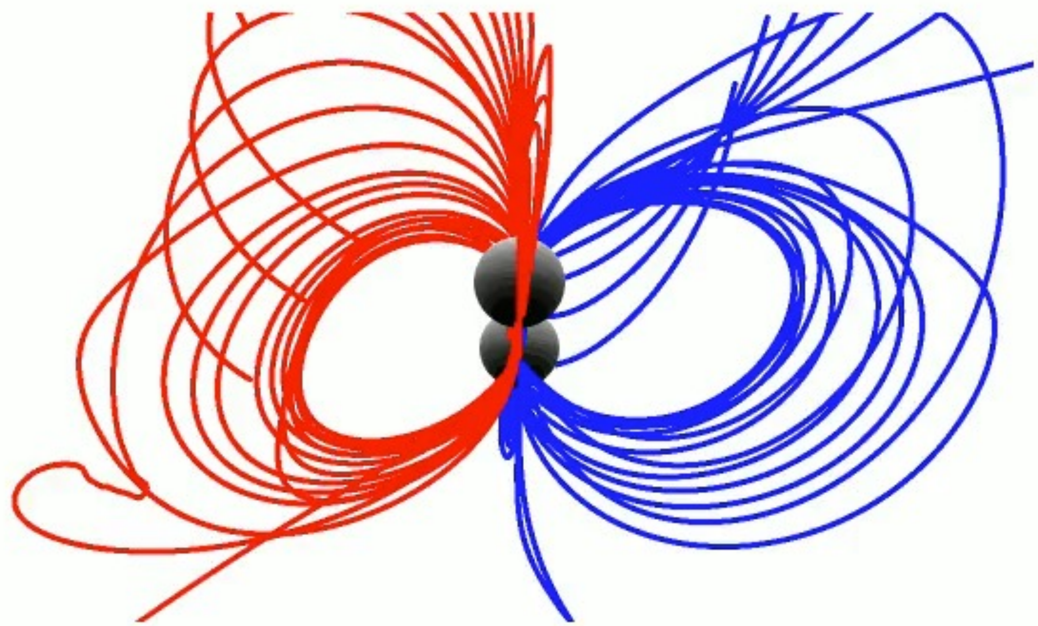

dimitrios.skiathas@nasa.gov

Aligned

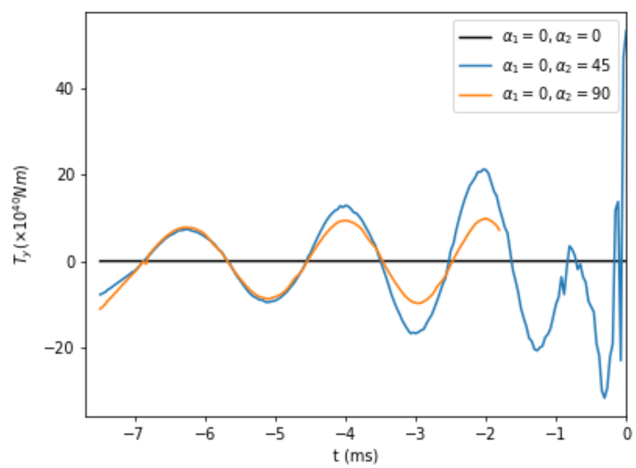

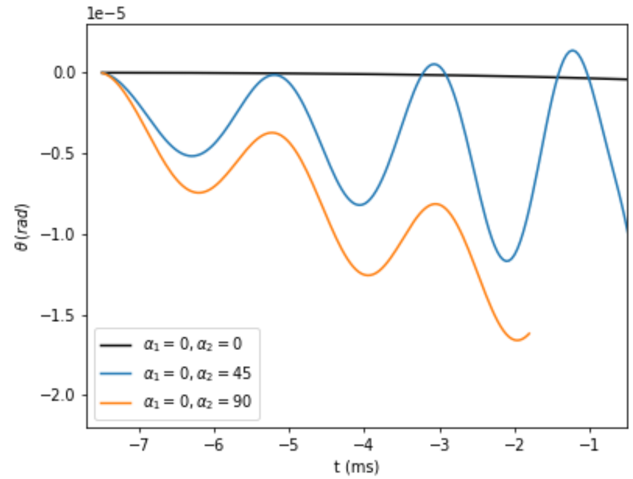

Anti-Aligned